 doi:10.20944/preprints202101.0444.v1

Letter

Analysis of Ocean Bottom Pressure Anomalies and Seismic Activities in MedRidge Zone

Hakan S. Kutoglu [1] and Kazimierz Becek [2,*]

[1] Zonguldak Bulent Ecevit University, Geomatics Engineering, Zonguldak, 67100, Turkey; shakan.kutoglu@beun.edu.tr
[2] Wroclaw University of Science and Technology, Geoengineering, Mining and Geology, Wroclaw, 50-357, Poland; kazimierz.becek@pwr.edu.pl
* Correspondence: kazimierz.becek@pwr.edu.pl; Tel.: +48 884670998

Abstract: Mediterranean Ridge accretionary complex (MAC) is one of the most critical subduction zones in the world. It is known that the region exhibits a continuous mass change (horizontal/vertical movements). This process is associated with the devastating and tragic earthquakes shaking the MAC for centuries. Here, we investigate the ocean bottom pressure (OBP) anomalies in the MAC derived from the Gravity Recovery and Climate Experiment (GRACE) and GRACE Follow On (GRACE-FO) satellite missions. The OBP time series for the MAC comprises a decreasing trend in addition to 1-, 1.53-, 2.36-, 3.67-, and 9.17-year periodic components partially explained by the atmosphere, oceans, and hydrosphere (AOH) processes, and Earth's pole movement. We noticed that the OBP anomalies appear to link to a rising trend and periods in earthquakes' power time series. This finding sheds new light on the mechanisms controlling the most destructive natural hazard.

Keywords: GRACE; Ocean Bottom Pressure; Earthquakes; Mediterranean Ridge accretionary complex.

1. Introduction

The satellite gravimetry technique has been developed for measuring gravity anomalies across the Earth. The gravity anomalies are caused by mass variations, including those in the ocean basins. The ocean basin mass variations are linked to changes in the hydrostatic pressure at the seafloor [1]. This hydrostatic pressure at the seafloor is known as the ocean bottom pressure (OBP). The OBP is the combined pressure caused by the column of seawater's weight and the atmosphere above the seafloor [2]. Hence, the OBP can be derived from the gravity anomaly data [3,4].

The OBP variations are driven by (i) air masses pressure; (ii) changes in ocean water mass due to an inflow of water from the continents and regional redistribution due to attraction effects of external masses located at the continents and in the atmosphere; and (iii) the redistribution of water within the ocean basins in response to atmospheric surface winds, atmospheric surface pressure gradients, and ocean thermohaline effects (i.e., the general ocean circulation) [5,6], [1], [7–10].

Plate tectonics is a distinctive source of mass change in the Earth's lithosphere. Especially, divergent and convergent plate boundaries are the places where continuous mass changes occur. A divergent boundary is an area where two plates are moving apart, and a new crust is created by magma pushing up from the mantle. A convergent boundary is an area where the plates move towards each other. When two plates meet each other, the thinner, denser, and more flexible one subducts under the other. As a result, a mass change (horizontal/vertical movements) around the subduction boundary [11–15]. Briefly, mass change in the divergent and convergent plate boundaries are reflected in OBP variations.

In this study, we investigate a link between earthquake activities and OBP anomalies. The area of interest (AOI) is the Mediterranean Ridge (MAC) accretionary complex - one

Preprints (www.preprints.org) | NOT PEER-REVIEWED | Posted: 22 January 2021 doi:10.20944/preprints202101.0444.v1

of the most critical ocean bottom subduction zones globally, covering an area 300 km wide and 2000 km long. We use the OBP data from the database of the GRACE and GRACE-FO satellite missions.

2. Materials and Methods

The Mediterranean Ridge accretionary complex is an arc-shaped wedge located on the Eastern part of the Mediterranean seafloor. The MAC is formed by the African Plate's collision with the Eurasian Plate [16], [17], [18]. The MAC consists of three parts: the outer, the inner parts, and Hellenic trenches. Figure 1 illustrates the location of MAC.

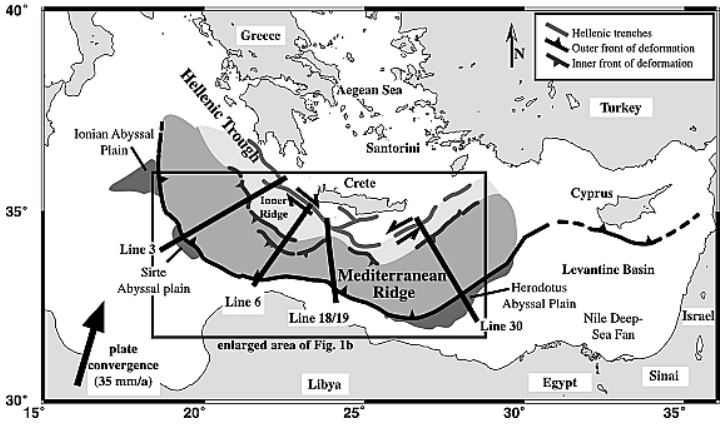

Figure 1. Location of the MAC in the eastern Mediterranean sea basin. The arrows indicate the present plate kinematic direction and rate between Africa and Eurasia [19,20].

The African Plate in MAC subducts beneath the Eastern European plate with the relative velocity of approx. 3.5 cm/year [21–26]. The subduction zone of the MAC experience a systematic mass change. This ridge system frequently produces major earthquakes, sometimes associated with tsunami events [27–28]. Figure 2 shows the earthquakes > M6 that occurred in MAC since 1970.

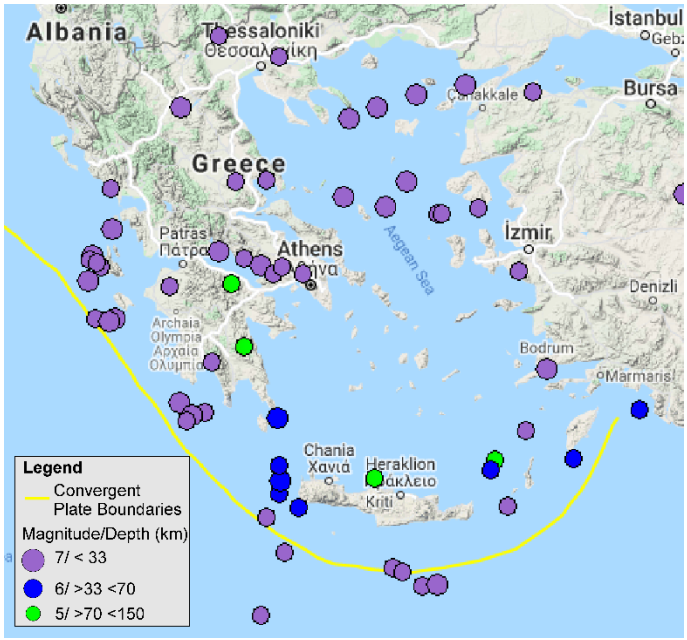

Figure 2. Earthquakes occurred since 1970 in MedRidge Zone. Source: [29].

OBP estimates were obtained from the GRACE and GRACE-FO mission [3,4]. The data can be downloaded from [30]. The spatial resolution is 1° x 1°, and the temporal resolution is one month, except for some missing records. Consequently, on average, seven

Preprints (www.preprints.org) | NOT PEER-REVIEWED | Posted: 22 January 2021 doi:10.20944/preprints202101.0444.v1

records/year are available in the dataset. The data cover the period from April 4, 2002, to October 25, 2017 (GRACE mission), and from June 1, 2018, to July 1, 2020 (GRACE-FO mission), which results in a seven-month-long gap in the OBP time series. The OBP data available at the source was altered by removing the time-average OBP value calculated from January 2003 and December 2007 period [30].

Figure 3 shows a map of a section of the Mediterranean Sea, including the MAC region. Over 200 earthquakes (M ≥ 5) locations are marked with black crosses. The OBP anomalies are shown as a background map. A spatial association between the OBP anomalies and the location of earthquakes is apparent in the MAC region.

For a detailed investigation of the OBP anomalies, we selected 14 earthquake locations (M ≥ 6) that recently occurrences in the MAC. They are shown in Figure 3 as red dots. The time series of the OBP anomalies for the 14 locations are shown in Figure 4. The OBP anomalies are consistent, except for one location. The outstanding location belongs to the North Anatolian fault Zone (NAFZ) and not MAC.

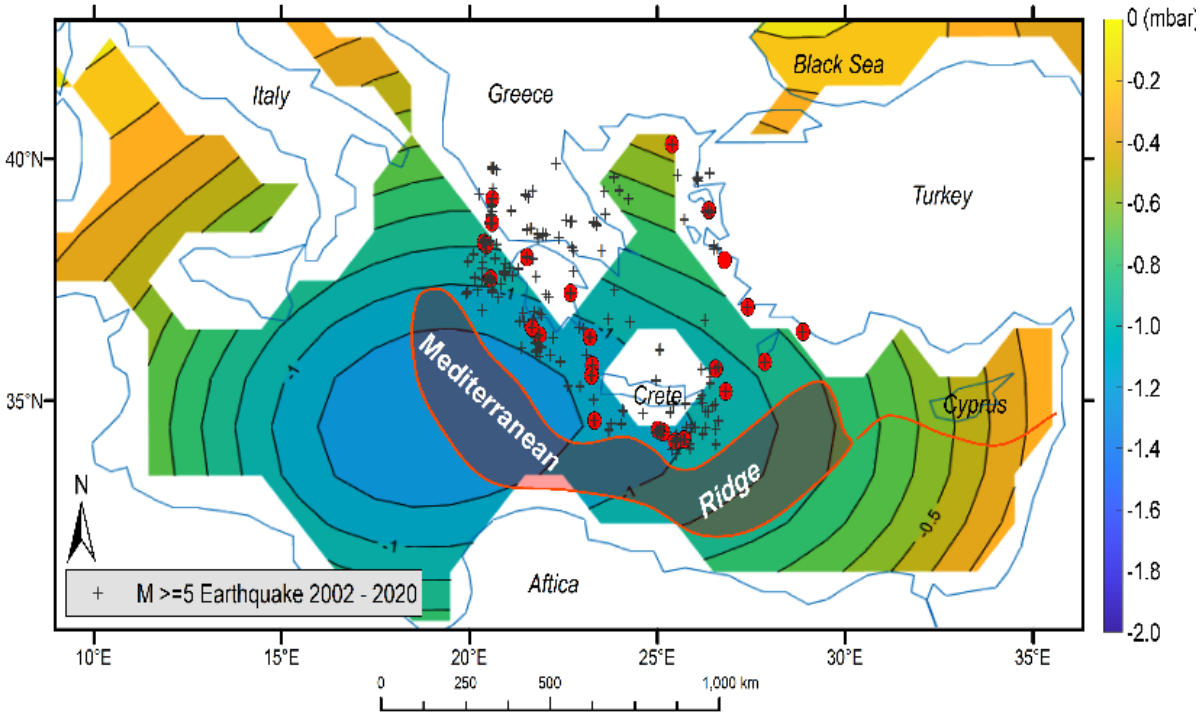

Figure 3. Map of the OBP in the MAC region, location of earthquakes (M ≥ 5) occurred in the area from 2002 to the present. The red dots are M ≥ 6 earthquake locations selected for detailed study.

Preprints (www.preprints.org) | NOT PEER-REVIEWED | Posted: 22 January 2021 doi:10.20944/preprints202101.0444.v1

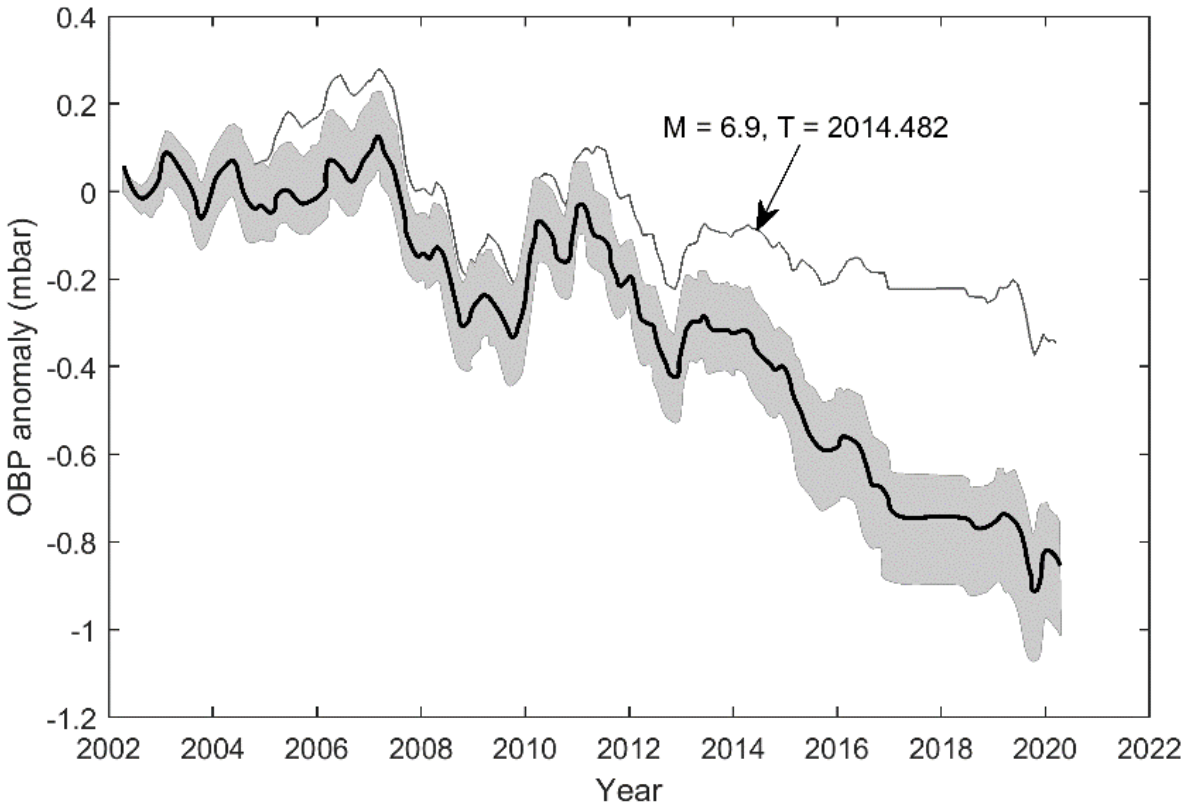

Figure 4. OBP anomaly range for 14 selected earthquake locations. A solid black line indicates a time-averaged OBP anomaly time series for the selected locations. The outstanding plot represents the OBP anomaly data for the M = 6.9 earthquake location (40.29N, 25.39E) at the 2014.482 epoch. This location belongs to the North Anatolian fault Zone (NAFZ).

3. Results

The OBP time series contain a decreasing trend and oscillations. To model the OBP anomalies, we first resampled the OBP time series to a uniform sampling rate of 12 samples/yr. In the next step, we detrend the time series using the piecewise linear function found in MatLab. As breakpoints, Jan. 2003 and Dec. 2017 were selected. This is because records between Jan. 2003 and Dec. 2007 were time-averaged, and the average OBP value was extracted from the data. Figure 5 (left pane) shows the OBP time series, the trend, and the resulting detrended OBP time series. To filter out high-frequency data, we used the low-pass Butterworth filter. Using the Fast Fourier Transform (FFT) algorithm, we identified 9.17-, 3.67-, 2.3-, 1.53-, and 1.02-year periods in the detrended OBP time series. Figure 5 (right pane) shows the power spectrum density of the detrended OBP time series.

Preprints (www.preprints.org) | NOT PEER-REVIEWED | Posted: 22 January 2021 doi:10.20944/preprints202101.0444.v1

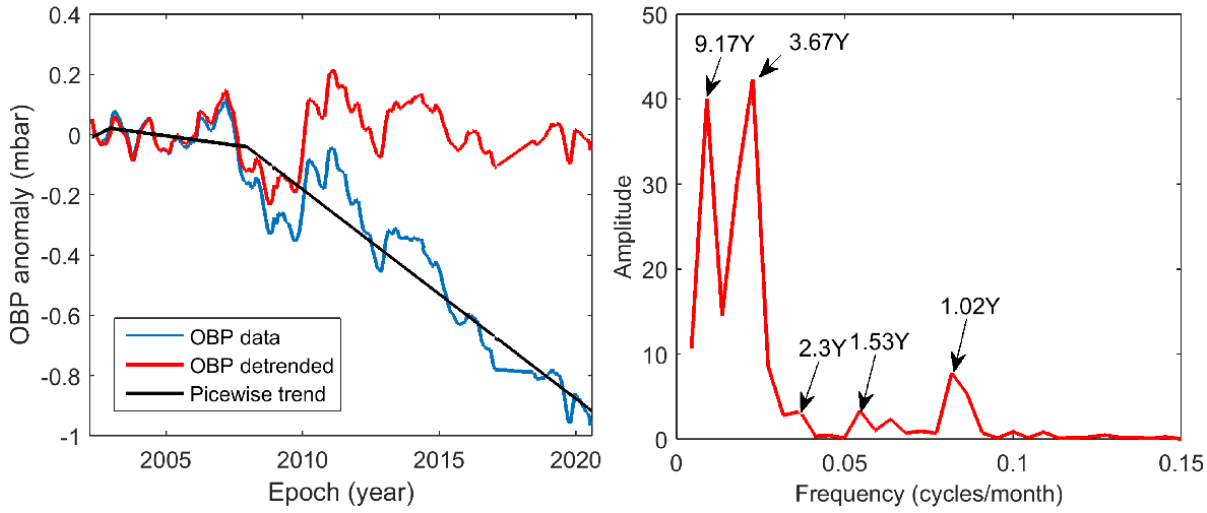

(**a**) (**b**)

Figure 5. (**a**) OBP time series (blue line), piecewise trend (black line), and detrended OBP time series (red line). (**b**) Power spectrum density of the detrended OBP time series.

Here, we attempt to link the OBP anomalies trend with the tectonic activities in the MAC zone. To this end, we investigate a time series of the power of earthquakes recorded in the MAC zone. We use equation (1) to convert earthquake magnitude into energy:

$$logE = 5.24 + 1.44M, \quad (1)$$

where E is in (J).

We summarise the energy in one-year bins. Figure 6 shows the time series of (M ≥ 5) earthquakes' power in annual intervals from 2002 to 2020 in the MAC zone. A clear rising trend in the power of earthquakes is visible. Some local extremes are also present in 2008, 2014, and 2020 years, suggesting a certain periodicity.

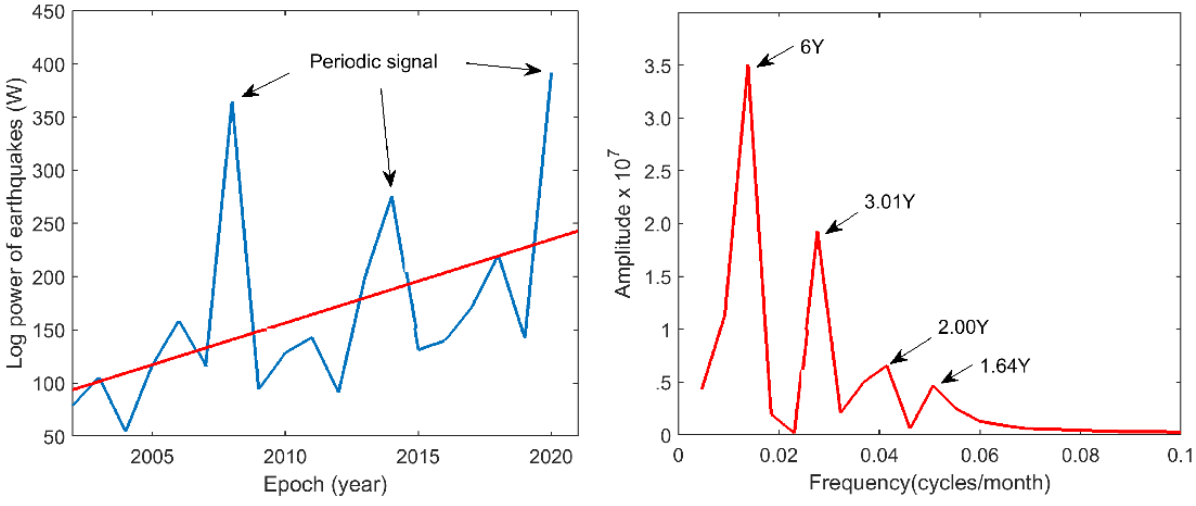

(**a**) (**b**)

Figure 6. (**a**) Time series of the (M≥5) earthquakes' power, including linear trend. Periodic components appear to present as well. (**b**) The periodogram of the earthquake power time series is shown in the right pane.

4. Discussion

A close study of Fig. 3 concludes that a significant OBP anomaly is present in the MAC zone's western section. Such a prominent feature is not observed outside of the

MAC region. This part of the ocean floor subducts under the continental part in the MAC zone's eastern section. Therefore, a long-term decrease in the OBP anomaly in the region is anticipated because of the constant mass change.

The time-series analysis yields a prominent decreasing trend and 1.02, 1.53, 2.3, 3.67, and 9.17-year oscillations in the OBP variations. The AOH processes play a dominant role in Earth's dynamic process for seasonal and interannual periods up to 4 years [31]. In this respect, the 1.02, 1.53, 2.3-year oscillations are evaluated to be caused by AOH processes. Longer oscillations and a linear trend in the dynamic processes of the Earth are believed to be caused by a combination of geophysical causes such as a slow rebound of the crust and upper mantle [32,33], and decadal angular momentum exchange between core and mantle [34–39]. Based on this expression and the MAC's geological settings, the linear decreasing trend and 9.17-year oscillation period of the OBP can be explained by the subduction tectonic process in the MAC Zone.

To investigate the hypothesis that tectonic interactions in the MAC zone drive the long-term OBP variations, we compiled a time series of the annual released power of earthquakes $M \geq 5$ for the AOI. The earthquakes' power time series features a rising trend and a periodic component. The increasing trend of the earthquake energy is consistent with the decreasing trend of the OBP and support the hypothesis that the tectonic process mainly drives the long-term OBP variation in the MAC Zone. The earthquakes' power time series includes four oscillations with 6, 3.01, 2, and 1.64 year periods. Tectonic processes drive the six-year oscillation. The periods 1.64, 2.00, and 3.01 years are similar to those in the OBP and probably driven by AOH forces.

5. Conclusions

MedRidge is one of the most critical subduction zones in the world. This fault system produced earthquakes > M8 that devastated the ancient cities in the region. However, such an earthquake has not been experienced for centuries. The OBP time series from GRACE and GRACE-FO satellite platforms show that the OBP around the MAC Zone drastically goes down. According to the literature, mass redistribution in mantle and crust are among the possible reasons for OBP variation. Linear trend and 9.17-year oscillation period in the OBP data point out the effect of the subduction tectonic process in the MAC Zone. The increasing linear trend of the earthquake energy released also supports this hypothesis. The MAC has the potential to produce devastating earthquakes. Therefore, the OBP variation in the region must be studied with longer records to understand better the relationship between OBP and tectonic processes in the zone.

Author Contributions: H.S.K. conceived the experiment, H.S.K. and K.B. conducted the experiment, and H.S.K. and K.B. analyzed the results. H.S.K. wrote the original version. K.B. edited the text. All authors reviewed the manuscript.

Funding: This research received no external funding.

Acknowledgments: The authors thank Estimating the Circulation and Climate of the Ocean (ECCO) Project Consortium and JPL NASA for the OBP data.

Conflicts of Interest: The authors declare no conflict of interest.

References

1. Dobslaw, H.; Boergens, E.; Dill, R. COST-G GravIS RL01 ocean bottom pressure anomalies. V. 0002. GFZ data services. Available online: https://dataservices.gfz-potsdam.de/gravis/showshort.php?id=escidoc:5219908 (accessed on 19/01/2021. DOI: http://doi.org/10.5880/cost-g.gravis_01_l3_obp.
2. Poropat, L.; Dobslaw, H.; Zhang, L.; Macrander, A.; Boebel, O.; Thomas, M. Time variations in ocean bottom pressure from a few hours to many years: In situ data, numerical models, and GRACE Satellite Gravimetry. *J. Geophys. Res. Oceans*, **2018**, *123*, 5612–5623, DOI: https://doi.org/10.1029/2018JC014108.
3. Fukumori, I. A partitioned Kalman filter and smoother. *Mon. Wea. Rev.* **2002**, *130*, 1370–1383, DOI: https://doi.org/10.1175/1520-0493(2002)130<1370:APKFAS>2.0.CO;2.

4. Kim, S.B.; Lee, T.; Fukumori, I. Mechanisms controlling the interannual variation of mixed layer temperature averaged over the Niño-3 Region. *J. Climate*, **2007**, *20*, 3822-3843, DOI: 10.1175/JCLI4206.1.
5. Bingham, R.J.; Hughes, C.W. The relationship between sea-level and bottom pressure variability in an eddy-permitting ocean model. *Geophys. Res. Let*. **2008**, 35, L03602, DOI: https://doi.org/10.1029/2007GL032662.
6. Chambers, D.P. Evaluation of new GRACE time-variable gravity data over the ocean. *Geophys. Res. Let*. **2006**, *33*, L17603, DOI: https://doi.org/10.1029/2006GL027296.
7. Milburn, H.; Nakamura, A.; Gonzalez, F. Real-time tsunami reporting from the deep ocean. In OCEANS 96 MTS/IEEE Conference, Proceedings of the Coastal Ocean - Prospects for the 21st Century, Fort Lauderdale, FL. September 1996; 390–394.
8. Ponte, R.M.; Stammer, D.; Marshall, J. Oceanic signals in observed motions of the Earth's pole of rotation. *Nature*, **1998**, *391(6666)*, 476–479, DOI: https://doi.org/10.1038/35126.
9. Ray, R.D. Precise comparisons of bottom-pressure and altimetric ocean tides. *J. Geophys. Res. Oceans*, **2013**, *118*, 4570–4584, DOI: https://doi.org/10.1002/jgrc.20336.
10. Ray, R.D.; Erofeeva, S.Y. Long-period tidal variations in the length of day. *J. Geophys. Res. Solid Earth*, **2014**, *119*, 1498–1509, DOI: https://doi.org/10.1002/2013JB010830.
11. Frankel, H. The Continental Drift Debate. In *Scientific controversies: Case studies in the resolution and closure of disputes in science and technology*, Engelhardt Jr, H.T.; Caplan, A.L.; Eds.; Cambridge University Press: 1987.
12. Condie, K.C. *Plate tectonics and crustal evolution*, Butterworth-Heinemann: 1997, pp. 288. DOI: https://doi.org/10.1016/B978-0-7506-3386-4.X5000-9.
13. Meissner, R. *The Little Book of Planet Earth*, Copernicus Books: New York, USA, 2002.
14. Schubert, G.; Turcotte, D.L.; Olson, P. *Mantle convection in the Earth and planets*, Cambridge University Press: 2001.
15. Turcotte, D.L.; Schubert, G. *Plate Tectonics. Geodynamics*, Cambridge University Press: 2002.
16. Emery, K.O.; Heezen, B.; Allan, T.D. Bathymetry of the Eastern Mediterranean sea. *Deep-Sea Res*. **1966**, *13*,173–192, DOI: https://doi.org/10.1016/0011-7471(66)91098-9.
17. Heezen, B.C.; Ewing, M. The Mid Oceanic Ridge. In *The Seas,* Hill, M.N.; Ed.; Interscience: New York 1963, pp. 388–410.
18. Huguen, C.; Chamot-Rooke, N.; Loubrieu, B.; Mascle, J. Morphology of a pre-collisional, salt-bearing, accretionary complex: The Mediterranean Ridge (Eastern Mediterranean). *Mar. Geophys. Res*. **2006**, *27*, 61–75, DOI: https://doi.org/10.1007/s11001-005-5026-5.
19. Huguen, C. Volcanisme boueux et déformation récente à actuelle au sein de la Ride Méditerranéenne, d'après les données de la campagne PRISMED II. Available online: http://geologie-alpine.ujf-grenoble.fr/articles/GA_1999__75__135_0.pdf (accessed on 19/01/2021).
20. Kopf, A.; Mascle, J.; Klaeschen, D. The Mediterranean Ridge: A mass balance across the fastest growing accretionary complex on Earth. *J. Geophys. Res*. **2003**, 108, B8, 2372, https://doi.org/10.1029/2001JB000473.
21. Dewey, J.F.; Şengör, C. Aegean and sur-rounding regions: complex multiplate and continuum tectonics in a convergent zone. *Geol. Soc. Am. Bull*. **1979**, *90*, 84–92, DOI: https://doi.org/10.1130/0016-7606(1979)90<84:AASRCM>2.0.CO;2.
22. Kreemer, C.; Chamot-Rooke, N. Contemporary kinematics of the southern Aegean and the Mediterranean Ridge. *Geophys. J. Intl.* **2004**, *157*, 1377–1392, DOI: 10.1111/j.1365-246X.2004-02270.x.
23. Le Pichon, X.; Chamot-Rooke, N.; Lallemant, S.; Noomen, R.; Veis, G. Geodetic determination of the kinematics of central Greece with respect to Europe: Implications for Eastern Mediterranean tectonics. *J. Geophys. Res*. **1995**, *100(B7)*, 12675–12690.
24. McClusky, Balassanian, S.; Barka, A.; Demir, C.; Ergintav, S.; Georgiev, I.; Gurkan, O.; Hamburger, M.; Hurst, K.; Kahle, H.; Kastens, K.; Kekelidze, G.; King, R.; Kotzev, V.; Lenk, O.; Mahmoud, S.; Mishin, A.; Nadariya, M.; Ouzounis, A.; Paradissis, D.; Peter, Y.; Prilepin, M.; Reilinger, R.; Sanli, I.; Seeger, H.; Tealeb, A.; Toksöz, M.N.; Veis, G. Global positioning system constraints on plate kinematics and dynamics in the eastern Mediterranean and Caucasus, *J. Geophys. Res*. **2000**, *105*, 5695–5719, DOI: https://doi.org/10.1029/1999JB900351.
25. Olivet, J.L.; Bonnin, J.; Beuzart, P.; Auzende, J.M. Cinématique des plaques et paléogéographie: une re-vue, *Bull. de la Société Géologique de France* **1982,** *XXIV*, 875–892, DOI: https://doi.org/10.2113/gssgfbull.S7-XXIV.5-6.875.
26. Reillinger, R.E.; McClusky, S.C.; Oral, M.B.; King, R.W.; Toksoz, M.N.; Barka, A.A.; Kinik, I.; Lenk, O.; Sanli, I. Global positioning system measurements of present-day crustal movements in the Arabia-Africa-Eurasia plate collision zone. *J. Geophys. Res. Solid Earth*, **1997**, *102*, 9983–9999. DOI: https://doi.org/10.1029/96JB03736.
27. Papadopoulos, G.A.; Papageorgiou, A. Large earthquakes and tsunamis in the Mediterranean and its connected seas. In *Extreme natural hazards, disaster risks, and societal implications*. Ismail-Zadeh, Alik, I-Z.; Fucugaughi, J.; Kijko, A.; Takeuchi, K.; Zaliapin, I.; Eds.; Cambridge University Press, 2014, pp. 252–266.
28. Papadopoulos, G.A.; Gràcia, E.; Urgeles, R,; Sallares, V.; De Martini, P.M.; Pantosti, D.; González, M.; Yalcinere, A.C.; Mascle, J.; Sakellariou, D.; Salamon, A.; Tinti, S.; Karastathis, V.; Fokaefs, A.; Camerlenghi, A; Novikova, T.; Papageorgiou, A. Historical and pre-historical tsunamis in the Mediterranean and its connected seas: Geological signatures, generation mechanisms and coastal impacts. *Mar. Geol*. **2014**, *354*, 81–109, DOI: https://doi.org/10.1016/j.margeo.2014.04.014.
29. IRIS earthquake browser. Available online: https://ds.iris.edu/ieb/index.html (accessed on 20/1/21).
30. JPL. ECCO Ocean Bottom Pressure (monthly). Available online: http://grace.jpl.nasa.gov (accessed on 20/1/21).
31. Chen, J.; Wilson, C.R.; Kuang, W.; Chao, B.F. Interannual oscillations in Earth rotation. *J. Geophys. Res. Solid Earth*, **2019**, *124*, DOI: https://doi.org/10.1029/.
32. Peltier, W.R. Global sea level and Earth rotation. *Science*, **1988**, *240(4854)*, 895–901, DOI: https://doi.org/10.1126/science.240.4854.895.

33. Wu, P.; Peltier, W.R. Pleistocene deglaciation and the Earth's rotation: A new analysis. *Geophys. J. Roy. Astron. Soc*. **1984**, *76(3)*, 753–791, DOI: https://doi.org/10.1111/j.1365-246X.1984.tb01920.x.
34. Buffett, B.A. A mechanism for decade fluctuations in the length of day. *Geophys. Res. Let*. **1996**, *23(25)*, 3803–3806, DOI: https://doi.org/10.1029/96GL03571.
35. Hide, R.; Clayton, R.W.; Hager, B.H.; Spieth, M.A.; Voorhies, C.V. Topographic core-mantle coupling and fluctuations in the Earth's rotation. In *Relating geophysical structures and processes: The Jeffreys volume, Geophysical Monograph Series* Aki, K.; Dmowska, R.; Eds.; American Geophysical Union, Washington DC, USA, 1993; Volume 76, pp. 107–120.
36. Jault, D.; Gire, C.; Le Mouel, J.L. Westward drift, core motions, and exchanges of angular momentum between core and mantle. *Nature*, **1988**, *333(6171)*, 353–356. https://doi.org/10.1038/333353a0.
37. Kuang, W.; Chao, B. F. Geodynamo modeling and core-mantle interactions. In *Earth's core: Dynamics, structure, rotation, geodynamics series*, Dehant, V.; Kreager, K.; Karato, C.; Zatman, S.; Eds.; American Geophysical Union: Washington DC, USA, 2003; Volume 31, pp. 193–212.
38. Mound, J.E.; Buffett, B.A. Interannual oscillations in length of day: Implications for the structure of the mantle and core. *J. Geophys. Res*. **2003**, *108*, 2334, https://doi.org/10.1029/2002JB002054.
39. Mound, J.E.; Buffett, B.A. Mechanisms of core-mantle angular momentum exchange and the observed spectral properties of torsional oscillations. *J. Geophys. Res*. **2005**, *110*, B08103, https://doi.org/10.1029/2004JB003555.